An Analysis of Exhaust Emissions from a Large Ship Docked in Humboldt Bay.

Cameron Bracken
Anthony Carnemolla
Colin Ritter
Eric Zielke, EIT

Submitted To:
Dr. Charles Chamberlin

ENGR 416 - Transport Phenomena
12-05-07

Abstract

This project examined the hypothetical situation of a large ship berthed in Humboldt Bay, CA. PM_{10} emitted by both auxiliary and main engines was considered. A 2-D finite element model and a 3-D Guassian plume model were developed to evaluate potential far field violations of the EPA's PM_{10} standard that may occur in and around the City of Eureka, CA. One year of hourly meteorological data was used to calculate model parameters. The finite element model failed due to instability under the range of dispersion coefficients calculated. With the Gaussian plume model and the emissions of a typically sized auxiliary engine we determined that no 24 hour violations would occur over the course of a year. The minimum mass flux of PM_{10} to cause a single violation was 350 times larger than a typical auxiliary ship engine. The Gaussian model was most sensitive to the the actual stack height. The actual stack height directly influences the effective stack height and thus the concentration of PM_{10} at ground level.

Contents

List of Figures

List of Tables

1 Introduction

Emissions from marine vessels raise concerns about the health of humans within close proximity of bays and harbors. Marine vessels contain a wide variety of diesel engines generally categorized as either a main or an auxiliary engine. Both of these engines emit a large variety of contaminants known to be harmful to humans when exposure limits are exceeded [USEPA 1995]. Specifically, particulate matter with a diameter less than 10 μm (PM_{10}) can cause many adverse health effects. A dose response curve is included in Appendix D.

Humboldt Bay is located roughly 350 miles north of San Francisco, CA and is California's second largest natural bay. Although Humboldt Bay is not a major port (i.e. capacity over 100 berths), it has potential for growth and, therefore, potential to harbor a large number of ships. This paper examines the hypothetical situation of a large ship berthed in Humboldt Bay. PM_{10} emitted by both auxiliary and main engines is considered. Both a 2-D Finite Element model and a 3-D Guassian Plume model are developed to determine potential far field violations of California's EPA PM_{10} standards that may occur in and around the City of Eureka, CA. Using hourly meteorological observations from the Arcata/Eureka Airport, the contaminant plume from a docked ship is modeled over the course of a year. Ground level violations of the EPA standard for PM_{10} at locations within 35 kilometers from the source are counted, allowing their frequency and location to be charted.

The parameters considered for the model are the exit height and diameter of the exhaust smoke stack on the ship, the exhaust velocity and temperature, and the concentration of PM_{10} in the exhaust. Also considered are the meteorological data such as insolation, cloud cover, cloud ceiling, and wind speed and direction. The exhaust flow rate, temperature and PM_{10} concentration parameters are largely dependent on the ship's engine power rating, where a more powerful engine will generally be larger and consequently will emit more of the contaminant. The California EPA's air quality standard requires the PM_{10} concentration to not exceed 50 $\mu g/m^3$, averaged over a 24-hour time period [ARB 2007].

1.1 Statement of Objectives

This project's objectives are detailed as follows,

- Determine if a constantly running auxiliary engine on a docked ship in the Humboldt Bay would violate the California EPA's 24 hour PM_{10} standard.
- Model and perform a sensitivity analysis of PM_{10} violations based on mass flux at stack tip, effluent exit temperature, effluent exit velocity, stack diameter, stack height, and meteorological data from the Arcata/Eureka Airport (ambient temperature, wind speed, wind direction, cloud cover).
- Determine where and how frequently violations occur.
- Analyze the conditions under which violations occur.

2 Literature Review

The objective of this literature review is to survey the factors that influence exhaust plume contaminants from docked ships. The problems associated with the contaminant plumes from docked ships are discussed. This is followed by a background on the mechanics of atmospheric dispersion, and finally a discussion of the analytical and numerical techniques that have been used to analyze contaminant transport.

2.1 Fuel Contaminants, PM_{10}, and Human Health

A wide range of fuel contaminants are emitted by engine exhaust, such as: nitrogen oxides (NO_X), sulphur dioxide, carbon monoxide, hydrocarbons, carbon dioxide, particulate matter (PM), and polyaromatic hydrocarbons [Cooper 2003]. PM_{10} (particulate matter that measures 10 μm or less) is composed of a wide variety of compounds and impurities. PM_{10} is easily inhaled deep into human lung tissue and long term exposure can lead to a host of adverse human health effects [UKNEAI 2007]. These effects range from coughs, asthma symptoms, bronchitis, respiratory illness and even mortality [Carbon 2003]. A dose response curve in Appendix D illustrates the risk of disease as a function of exposure to PM_{10}. The California EPA regulates PM_{10} with an Air Quality Standard (AQS) of 50 $\mu g/m^3$ on average for a 24-hour time period and 20 $\mu g/m^3$ on an annual average [ARB 2007].

2.2 Plumes from Docked Ships

Large sea vessels consume fossil fuel and emit particulate matter in their exhaust [Janhall 2007]. Large ships usually have two engines, a main and an auxiliary engine. The auxiliary engine is run continuously while a ship is docked to provide electricity.

Several studies have been conducted concerning the air quality effects of docked ships on port cities [Lua et al. 2006; Cooper 2003; Janhall 2007]. In a Vancouver study, Lua et al. [2006] argue that docked ships had a noticeable effect on inland (4-8 km) air quality 8 times in 15 days. Depending on the ship and engine type, PM matter is generally emitted at a concentration of 21-107 mg/m^3 of engine exhaust with a volumetric exhaust rate of 2620-7150 m^3/hr [Cooper 2003]. The current Best Available Control Technology for Toxics (TBACT) requirement for PM_{10} emission rates is 0.15g/bhp·hr. Given a particular emission rate, the mass flux of PM_{10} from the most contaminated plume may calculated as follows [BAAQMD 2007],

$$\dot{m}_{\mathrm{PM}_{10}} = Em \cdot \mathscr{P}_{\mathrm{eng}} \tag{1}$$

where

$$\begin{aligned} Em &= \text{Emission rate (g/bhp·hr)} \\ \dot{m}_{\mathrm{PM}_{10}} &= \text{Mass flux of } PM_{10} \text{ (g/hr)} \\ \mathscr{P}_{\mathrm{eng}} &= \text{Power of engine (bhp)} \end{aligned}$$

Table 2 in Appendix C provides calculated values of mass flux in comparison to values determined from field studies. The discharge velocity of exhaust plumes are largely dependent on the dimensions of the exhaust pipe. For example, one study suggested an exhaust pipe at a height of 45 m and 5 m in diameter exhibited a discharge velocity of 10 m/s [Kitabayashi et al. 2006]. Another study suggested exhaust exiting rates of 35-40 m/s with stack heights of 34 to 58 m and a stack diameter of 1.3 m [CSU 2007]. Exiting exhaust temperatures range from 273°C to 405°C [Cooper 2003]. With these given parameters, plumes emitted by ships have been detected at distances of 1 to 3 km downwind; however, the contaminants tend to deposit on the ground rapidly [Janhall 2007; Ninga et al. 2005].

2.3 Behavior of Atmospheric Plumes

2.3.1 Stability and Wind Speed Profiles

The amount of solar radiation, cloud cover, and surface wind speed can be used to classify the stability of the atmosphere [Turner 1970]. The respective categories range from extremely unstable to moderately stable and are called Pasquill's Stability Categories (Appendix B). The stability of the atmosphere and the terrain on the ground both influence the vertical wind speed profile. Plumes may be emitted at and rise to altitudes for which there is no wind speed data. In such times estimates can be made based on the wind speed power law [Gipe 2004].

$$u_2 = u_1 \left(\frac{z_2}{z_1} \right)^p \tag{2}$$

where

z_1 = height above ground at which wind speed is known (m)
z_2 = height above ground at which wind speed is unknown (m)
u_1 = wind speed at known height (m/s)
u_2 = wind speed at unknown height (m/s)
p = empirical constant (dimensionless)

The exponent p is dependent on the stability category and type of terrain. Table 2 in Appendix B provides commonly used values in rural and urban settings.

2.3.2 Plume Rise

A plume emitted from a stack may rise, fall, or stay roughly at the same height depending on the exit velocity of the gas, the diameter of the stack, the stack gas temperature, the ambient air temperature, and the stability category of the atmosphere [Altwicker 2000]. The height at which the plume stabilizes is called the effective stack height, which is assumed to equal the centerline of the plume. Briggs developed formulae to estimate the effective stack height under various conditions (Appendix A).

2.4 Advection-Dispersion Equation

The advection-dispersion (A-D) is a partial differential equation (PDE) widely used to model pollutant transport [Kitabayashi et al. 2006; Nepf 2004; Schwarz et al. 2006]. The three dimensional A-D equation for a conservative contaminant within a density independent flow field is

$$\frac{\partial C}{\partial t} + \nabla \cdot (\overline{\mathbf{u}} C) = \nabla^2 \cdot (\mathbf{D} C). \tag{3}$$

where $\overline{\mathbf{u}} = (\overline{u}_x, \overline{u}_y, \overline{u}_z)$ is the vector of average fluid speeds in the three spatial directions and $\mathbf{D} = (D_x, D_y, D_z)$ is the dispersion coefficient in each direction. The A-D equation, derived from a mass balance of a control volume [Socolofsky 2002], is used to model the simultaneous advection due to bulk fluid flow and dispersion due to a concentration gradient. The A-D equation has been applied to groundwater contamination [Mazzia et al. 2000], heat transfer [Tkalich and Chan 2003], and air quality modeling [Schwarz et al. 2006] among many applications. Plume models are a natural application of the A-D equation. Gaussian plume models, discussed below, are analytical solutions to the A-D equation.

For most applications, a one or two dimensional solution to the A-D equation is sufficient to model a transport process. In the case of atmospheric plume modeling, if conditions are stable then there is little or no vertical air movement and the vertical term in the A-D equation can be ignored if complete mixing over a fixed thickness is assumed. If constant wind speed is assumed along with constant diffusion, the A-D equation becomes

$$\frac{\partial C}{\partial t} + \overline{u}_x \frac{\partial C}{\partial x} + \overline{u}_y \frac{\partial C}{\partial y} = D_x \frac{\partial^2 C}{\partial x^2} + D_y \frac{\partial^2 C}{\partial y^2}. \tag{4}$$

For plume modeling, the solution to equation 3.2 describes the evolution of a continuous or slug point discharge over time.

2.5 Gaussian Plume Model

In a gaussian plume, the spatial distribution of concentration along a transverse axis is Gaussian in shape. The following steady state 3-dimensional model describes the concentration at any point in a coordinate system where the wind is moving parallel to the x-axis [Altwicker 2000].

$$\chi(x, y, z, h_e) = \frac{Q}{2\pi \sigma_y \sigma_z u_s} e^{\left(\frac{-y^2}{2\sigma_y^2}\right)} e^{\left(\frac{-(z-h_e)^2}{2\sigma_z^2}\right)} \tag{5}$$

where

χ = concentration of contaminant (g/m^3)
x, y, z = distance from origin in x, y, z coordinates (m)
h_e = effective stack height (m)
Q = rate of emission of gas (g/s)
σ_y, σ_z = horizontal and vertical plume standard deviations (m), each a function of x
u_s = wind speed at effective stack height (m/s)

The Gaussian model is an analytical solution to the 3D advection-dispersion equation with the following assumptions [Altwicker 2000]:

- Wind speed is constant,
- The system is at steady state,
- Diffusion in the x-direction is ignored and the other diffusion coefficients are anisotropic,
- The plume can be reflected from the ground when an image source is added and mass is conserved
- Contaminant is conservative,
- And, Gas is assumed to be ideal and inert.

The dispersion coefficients σ_y, σ_z are dependent on the stability of the atmosphere and the downwind distance x (Appendix B).

2.6 Numerical Methods

Analytical solutions to the advection-dispersion equation provide quick ways to model the general behavior of contaminant transport. In many cases the assumptions necessary for analytical solutions (Section 2.5) make such models inapplicable to real world situations. Numerical methods provide a means for solving more realistic complicated models of atmospheric dispersion over more irregular domains and varying boundary conditions. Two of the most common numerical methods used are finite differences and finite elements [Huebner et al. 2001].

Finite difference methods use a Taylor series expansion of the underlying governing equation to approximate the solution [Chapra and Canale 2006]. The spatial and/or temporal domain of the problem can be discretized into a set of evenly spaced nodes or points and the approximating series is defined for each node. Usually only the first few elements of the series are used. The remaining elements are truncated, resulting in some inherent error at each node. The approximating equations are solved simultaneously to yield the solution for every node in the system.

When a finite difference method is used to solve the convection-dispersion equation, extra errors can be introduced. When the assumptions of a homogeneous and isotropic medium are relaxed, the parameter **D** in equation 7 remains a multidimensional tensor, and the truncation error from the Taylor series expansion becomes significant. Lantz

[1971] showed that the result is equivalent to adding a "numerical diffusion" term. Correction terms have been used to cancel out the inherent error in finite difference methods [Genuchten and Gray 1978]. These methods have introduced other errors, and newer finite difference methods involving weighting of the various terms have been developed to minimize these deficiencies [Wang and Lacroix 1997]. To eliminate the numerical diffusion error altogether, the finite element method can be used since it does not rely on a Taylor series expansion.

Finite element methods discretize the domain of the problem into regions or elements with distinct geometry and endpoints. A function is developed for each element that approximates the governing equation anywhere within that element or on its boundary. When the equations for each element are made to agree with each neighboring element at the boundaries, the resulting system of equations can be solved simultaneously to give the solution for any point within the system [Chapra and Canale 2006]. The method of weighted residuals is used to find the equations that provide the best fit to the governing equation [Willis and Yeh 1987]. Because finite element methods are better than finite difference methods at handling situations with irregular geometry and heterogeneity, the method is common in modelling environmental transport equations [Willis and Yeh 1987]. Some examples of the use of finite elements in modelling atmospheric contaminant transport are Sayma and Betts [1997] and Liu and Leung [1997].

3 Model Formulation

The general goal in modeling emissions from a docked ship in Humboldt Bay is to quantify the number of PM_{10} violations which occur over the course of a year. The steps in the solution process for each hour are: (1) input weather data for one hour, (2) use the weather data to make the stability calculations and develop the heterogeneous dispersion estimates, (3) input dispersion coefficients to the finite element and/or gaussian plume models, (4) asses the steady state concentrations for possible violations, and (5) repeat the process for every hour of a year. The approach for evaluating the PM_{10} emissions from a docked ship in Humboldt Bay is shown in Figure 1. This section outlines these model components.

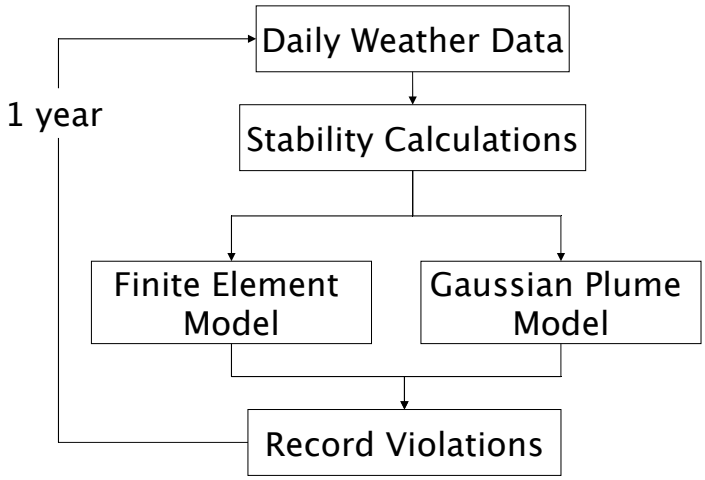

Figure 1: Modeling approach.

3.1 The Governing Equation

Density independent contaminant transport through an isotropic heterogeneous flow field is described by Fick's Law of Diffusion [Wang and Anderson 1982]. For a conservative constituent that is soluble in the flow field, the equation is

$$\underline{J} = -\nabla(\mathbf{D}\underline{C}) \tag{6}$$

where

$$\begin{aligned} \underline{J} &= \text{dispersive flux of contaminant } (\mathrm{g/m^2 \cdot s}) \\ \mathbf{D} &= \text{coefficient of dispersion } (\mathrm{m^2/s}) \\ \underline{C} &= \text{concentration of contaminant } (\mathrm{g/m^3}) \end{aligned}$$

Applying continuity principles to the dispersive flux yields the advection-dispersion (A-D) equation.

$$\nabla^2 \cdot (\mathbf{D}\underline{C}) - \nabla(\mathbf{u}\underline{C}) = \frac{\partial \underline{C}}{\partial t} \tag{7}$$

where

$\overline{\mathbf{u}}$ = average velocity of fluid through which the contaminant is moving
t = time

3.2 Finite Element Formulation

The A-D equation, assuming complete mixing in the vertical direction, is

$$\frac{\partial C}{\partial t} + \frac{\partial (uC)}{\partial x} + \frac{\partial (vC)}{\partial y} = \frac{\partial}{\partial x}\left(D_x \frac{\partial C}{\partial x}\right) + \frac{\partial}{\partial x}\left(D_y \frac{\partial C}{\partial y}\right).$$

where now u is the average velocity in the x direction, v is the average velocity in the y direction, and the z direction has been integrated out using Leibnitz's Rule [Willis and Yeh 1987].

What follows is a brief overview of the methods described in Wang and Anderson [1982] and elsewhere. Since the present application is isotropic, u, v, D_x and D_y can be factored out of the spatial gradients, and the governing equation becomes

$$\frac{\partial C}{\partial t} + u\frac{\partial C}{\partial x} + v\frac{\partial C}{\partial y} - D_x \frac{\partial^2 C}{\partial x^2} - D_y \frac{\partial^2 C}{\partial y^2} = 0.$$

To approximate the solution, the physical domain is discretized into small square domains called elements, and the four corners of the elements are called nodes. The general procedure requires finding solutions at each of the nodes and using interpolating functions to find solutions at every other place inside of each element. Figure 2 shows an archetypal square element with nodes i, j, m and n corresponding to the points (x_i, y_i), (x_j, y_j), (x_m, y_m) and (x_n, y_n).

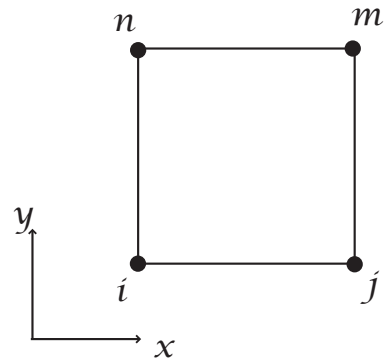

Figure 2: Archetypal element [Wang and Anderson 1982].

Next, an approximate solution of the contaminant concentrations can be found, $\tilde{C}(x,y,t)$, based on an interpolation function $N_L(x,y)$ and the solution C_L at each node L such that

$$\tilde{C}(x,y,t) = \sum_{L=1}^{\text{nnode}} C_L N_L(x,y) \tag{8}$$

where L is the node number, nnode is the total number of nodes. C_L is shorthand for $C(x_L, y_L, t)$.

Substituting in the approximate solution gives

$$\frac{\partial \tilde{C}}{\partial t} + u\frac{\partial \tilde{C}}{\partial x} + v\frac{\partial \tilde{C}}{\partial y} - D_x\frac{\partial^2 \tilde{C}}{\partial x^2} - D_y\frac{\partial^2 \tilde{C}}{\partial y^2} = R$$

where now the equation does not equal zero because $\tilde{C}$ is not exact. R is the global residual or error in the approximate solution. The method of weighted residuals provides a way to minimize the error at each node using a weighting function W_L for each node L such that

$$\iint_D R\, W_L\, dD = 0$$

where $L = 1, 2, ..., \text{nnode}$ and D is the entire problem domain. The Galerkin method uses the interpolation functions as the weighting functions, $W_L = N_L$, so that

$$\iint_D R\, N_L(x,y)\, dD = 0 \tag{9}$$

Equation 9 implies one equation for every node. Now substitute in for R

$$\iint_D \left(\frac{\partial \tilde{C}}{\partial t} + u\frac{\partial \tilde{C}}{\partial x} + v\frac{\partial \tilde{C}}{\partial y} - D_x\frac{\partial^2 \tilde{C}}{\partial x^2} - D_y\frac{\partial^2 \tilde{C}}{\partial y^2}\right) N_L(x,y)\, dD = 0 \tag{10}$$

Stokes theorem (a higher order version of integration by parts) is used to reduce the second order differential terms to first order,

$$\iint_D \frac{\partial^2 \tilde{C}}{\partial x^2} dD = -\iint_D \frac{\partial \tilde{C}}{\partial x}\,\frac{\partial N_L}{\partial x} dD + \int_{\partial s} \frac{\partial \tilde{C}}{\partial x}\, n_x\, N_L\, ds \tag{11}$$

where ∂s is the boundary of D, s is the distance around the boundary moving counterclockwise and n_x is the x component of the outward normal vector to the boundary of D. Substituting equation 11 into equation 10 for both of the second derivative terms gives

$$\iint_D \left(\frac{\partial \tilde{C}}{\partial t} N_L + \frac{\partial \tilde{C}}{\partial x} N_L + \frac{\partial N_L}{\partial x} N_L + \frac{\partial \tilde{C}}{\partial x}\,\frac{\partial N_L}{\partial x} + \frac{\partial \tilde{C}}{\partial y}\,\frac{\partial N_L}{\partial y}\right) dD = \int_{\partial s} \left(\frac{\partial \tilde{C}}{\partial x}\, n_x + \frac{\partial \tilde{C}}{\partial y}\, n_y\right) N_L\, ds \tag{12}$$

The approximate solution $\tilde{C}(x,y)$ using the interpolation functions over a single element has the form

$$\tilde{C}^e = C_i(t) N_i^e(x,y) + C_j(t) N_j^e(x,y) + C_m(t) N_m^e(x,y) + C_n N_n^e(x,y) \tag{13}$$

where e is the element number. The piecewise interpolation functions are required to be defined over a particular element, but equal zero everywhere else. Each function must equal 1 at its corresponding node and 0 at the other three nodes. A convenient set of interpolation functions for the quadrilateral element that satisfies all requirements is

$$N_i^e(x,y) = \frac{1}{4}\left(1-\frac{x}{a}\right)\left(1-\frac{y}{b}\right) \tag{14}$$

$$N_j^e(x,y) = \frac{1}{4}\left(1+\frac{x}{a}\right)\left(1-\frac{y}{b}\right) \tag{15}$$

$$N_m^e(x,y) = \frac{1}{4}\left(1+\frac{x}{a}\right)\left(1+\frac{y}{b}\right) \tag{16}$$

$$N_n^e(x,y) = \frac{1}{4}\left(1-\frac{x}{a}\right)\left(1+\frac{y}{b}\right) \tag{17}$$

$$2a = x_j - x_i = x_m - x_n \tag{18}$$

$$2b = y_n - y_i = y_m - y_j \tag{19}$$

Figure 3 shows the general shape and properties of a single interpolation function.

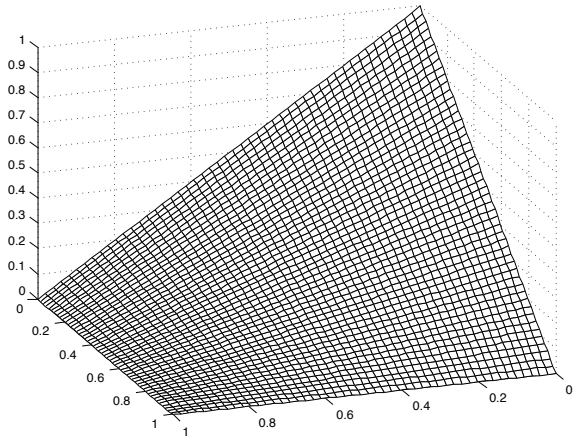

Figure 3: Interpolation function .

The representation of the solution based on the definition of the piecewise interpolation functions is

$$\sum_e \left[\iint_e \left(\frac{\partial \tilde{C}^e}{\partial t} N_L + \frac{\partial \tilde{C}^e}{\partial x} N_L + \frac{\partial N_L}{\partial x} N_L + \frac{\partial \tilde{C}^e}{\partial x} \frac{\partial N_L}{\partial x} + \frac{\partial \tilde{C}^e}{\partial y} \frac{\partial N_L}{\partial y} \right) dD \right] = \int_{\partial s} \left(\frac{\partial \tilde{C}}{\partial x} n_x + \frac{\partial \tilde{C}}{\partial y} n_y \right) N_L \, ds \tag{20}$$

The final step is to simultaneously solve all equations for all nodes within the domain of the problem. The integrations are made simple by using the gaussian quadrature method [Chapra and Canale 2006]. The result is a system of linear equations that is solved using Matlab's intrinsic sparse matrix routines and its left matrix divide function [MATLAB 2007].

3.3 Gaussian Plume Model

As described in Section 2, the Gaussian plume model is an analytical solution to the AD equation. The following 3-dimensional model describes the concentration at any point in a coordinate system where the wind is moving parallel to the x-axis [Altwicker 2000].

$$\chi(x, y, z, h_e) = \frac{Q}{2\pi\sigma_y\sigma_z u_s} e^{\left(\frac{-y^2}{2\sigma_y^2}\right)} e^{\left(\frac{-(z-h_e)^2}{2\sigma_z^2}\right)} \tag{21}$$

where

x, y, z	=	distance from origin in x, y, z coordinates (m)
h_e	=	effective stack height (m)
u_s	=	wind speed at stack height (m/s)
Q	=	rate of emission of gas (g/s)
σ_y, σ_z	=	horizontal and vertical plume standard deviations, functions of x (m)

For each set of meteorological observations, the Gaussian plume model was employed to calculate the concentration of PM_{10} at ground level out to a distance of 30km from the source.

3.4 Meteorological Data and Stability Calculations

The analytical gaussian plume model was combined with meteorological data to simulate the presence of a diesel engine at a Eureka dock over the course of a year. The data is available online from the Real-time Observation Monitoring and Analysis Network, a service of the National Weather Service [Horel et al. 2007]. A year's worth of hourly observations were downloaded including wind speed and direction, temperature, percent cloud cover, and cloud ceiling height. From these data, the atmospheric stability category is determined using Briggs' method (Appendix A). Plume rise formulae are then used to determine the final plume rise height. The dispersion coeffiecients and standard deviations are calculated (Appendix B) and finally the concentrations are determined.

Both the finite element and the Gaussian plume model are first solved as if all the wind were blowing along the x-axis. The solutions are then rotated about the source to simulate the true wind direction. The simulation assumes that the plume immediately comes to steady-state and remains there for the duration of that hour.

3.5 Violations

After the steady-state Gaussian solution was determined for a given hour, the average concentrations over the previous 24 hours were computed throughout the computational grid. These 24 hour average concentrations were compared to the EPA standard and the number of violations that occur at each point in the grid were noted. The resulting field of violation counts were plotted over a map of Eureka and the surrounding communities to investigate where the biggest impact is most likely to occur.

4 Application

To determine the number of violations that occur over the course of a year, a Matlab program was developed to calculate the concentration of PM_{10} over a square domain approximately 30 km across. Using data from descriptions of actual ship engines [Cooper 2003; CSU 2007], a set of representative parameters were determined to use as a base case scenario for the model (Table 1). Using these base case parameters, the number of days in a year in which a violation occurred was recorded. We call this number the "violation days." This metric was then used as a basis for comparison between successive model runs in the sensitivity analysis.

Table 1: Default model parameters used to investigate plume behavior.

Parameter	Description	Value	Units
$\dot{m}$	mass flux of PM_{10} at stack tip	350	g/hr
C^*	PM_{10} standard for a 24-hour time period	50	$\mu g/m^3$
d_s	stack tip diameter	1	m
T_s	effluent exit temperature	400	°C
v_s	stack exit velocity	30	m/s
terrain	terrain type	urban	n/a
h_s	stack tip height	40	m
$\Delta x, \Delta y$	grid resolution	850	m
z^*	height above ground at which concentrations were determined	0	m

4.1 Preliminary Results

4.1.1 Numerical Solution

The finite element model was developed and run successfully for a general case in which the magnitudes of the velocity terms are much smaller than the magnitudes of the dispersion terms in Equation 3.2. In this case, the finite element method is stable and generates the PM_{10} concentration at any point in the spatial domain at any point in time. Figure 4 shows an example of the output from the finite element model.

Unfortunately, these preliminary results could not be used to solve the actual problem of PM_{10} pollution in Humboldt Bay. As the magnitudes of the dispersion terms approach

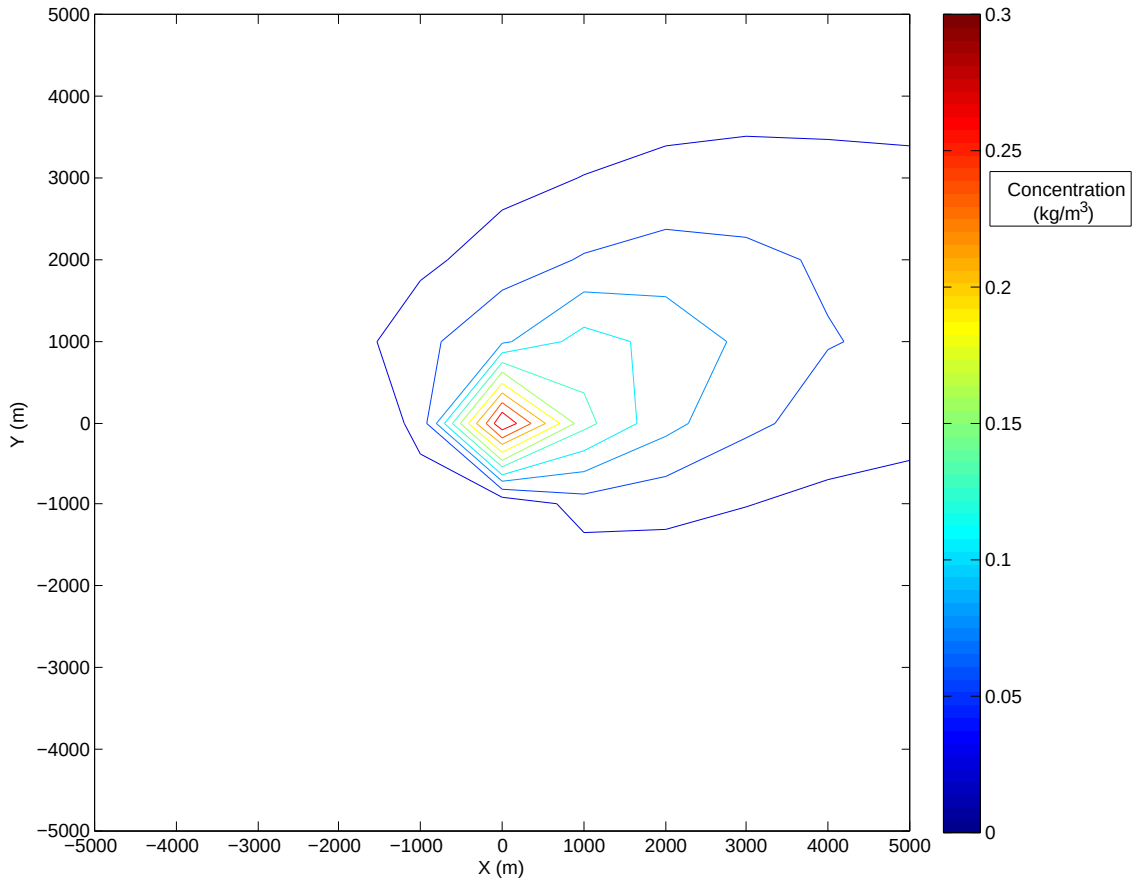

Figure 4: Example output from initial run of finite element model. $u = 20$ m/hr, $v = 10$ m/hr, $D_x = 20000$ m^2/hr, $D_y = 10000$ m^2/hr, $t = 225$ hr: smokestack at (0,0): 10000 kg/m^3·hr

the magnitudes of the velocity terms, the advection-dispersion equation becomes a hyperbolic equation [Willis 2007]. This was the case for the range of dispersion coefficients we calculated for Humboldt Bay. The result is that, with the actual parameters used in the current application, the model becomes unstable. This is a widely known problem with the basic finite element method in solving hyperbolic equations. Many variations on the basic finite element model have been developed to fix this issue of instability in hyperbolic equations [Calhoun-Lopez and Gunzburger 2005], but they were not attempted in the current study. The extremely erratic behavior of the finite element model prevented its use in solving the problem, and it prevented a comparison between the numerical model and the analytical gaussian plume model. The results shown in the next section will be from the analytical model only.

4.1.2 Restatement of Objectives

With the initial parameters specified above, we simulated the emissions from a ship over the course of 12 months using the Gaussian plume model. We found that there were

never any violations of the standard under these circumstances. The largest concentration of PM_{10} over a 24-hour time period at any point in the computational domain was about two orders of magnitude smaller than the standard.

To investigate the impact of a plume which does violate a standard in Humboldt Bay, we chose to vary the mass flux of PM_{10} to determine the minimum flux necessary to create violations. Therefore, the following results are for a hypothetical ship which has the same dimensions as the ship described above, but whose mass flux of PM_{10} is extremely large.

5 Results

Figures 5 and 6 show the concentrations calculated for 1 hour and averaged over 24 hours respectively. The plots were generated during a relatively high-concentration event when the atmospheric stability was stable and the wind speed was low.

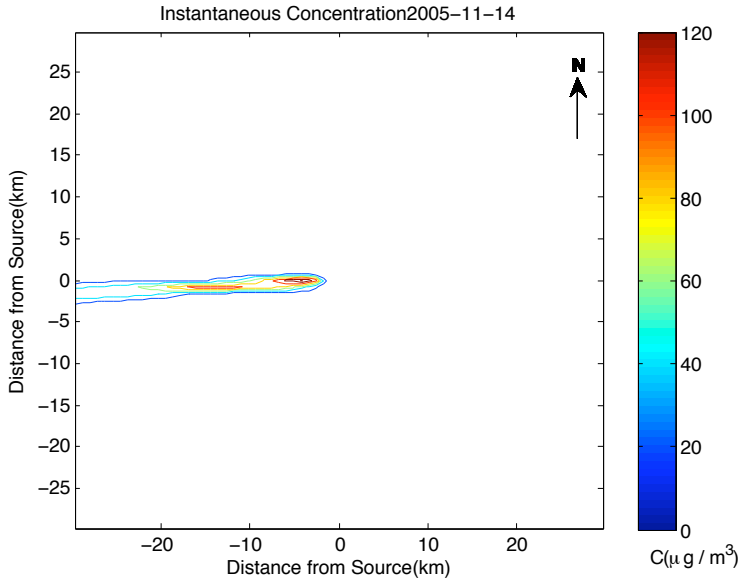

Figure 5: Isopleths of concentration of PM_{10} at ground level (z=0m) from the source at (0,0)km up to 30 km from the source at steady state during a relatively high concentration event.

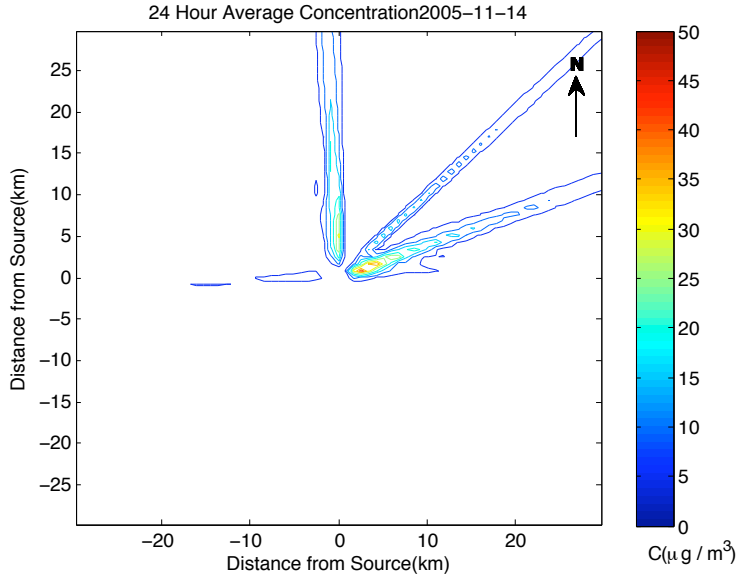

Figure 6: Average concentration isopleths at each point in the computational grid at ground level (z=0m) over a 24 hour time period.

The minimum mass flux of PM_{10} necessary to produce a violation of the standard is 122.5 kg/hr (Figure 7). This is an enormous quantity of PM_{10}, approximately 350 times larger than a typical auxiliary engine in a ship, and exceeds any quantity emitted from even a main ship engine [BAAQMD 2007; Cooper 2003]. While 122.5 kg/hr would not be a realistic mass flux for a single ship docked in Humboldt Bay, it is possible that many ships docked close together could emit such a quantity.

The violations at each point in the domain were counted over the course of a year and the resulting spatially distributed violation count was plotted over a map of Eureka, CA and the surrounding towns (Figure 8). One or more violations occurred over much of the City of Eureka, with violations of 100 or more occurring over 20-30 blocks in the north-west region of the city. Additionally, a region of the Samoa Peninsula experienced over 1000 violations close to the shoreline.

Northerly and southerly wind events do not produce violations. Because violations only occur when wind speeds are low, this observation may be attributable to a larger proportion of high wind speeds in the northerly and southerly directions. Alternatively, this may be attributable to a greater frequency of wind direction changes since violations tend to occur when the wind direction is close to constant over many hours.

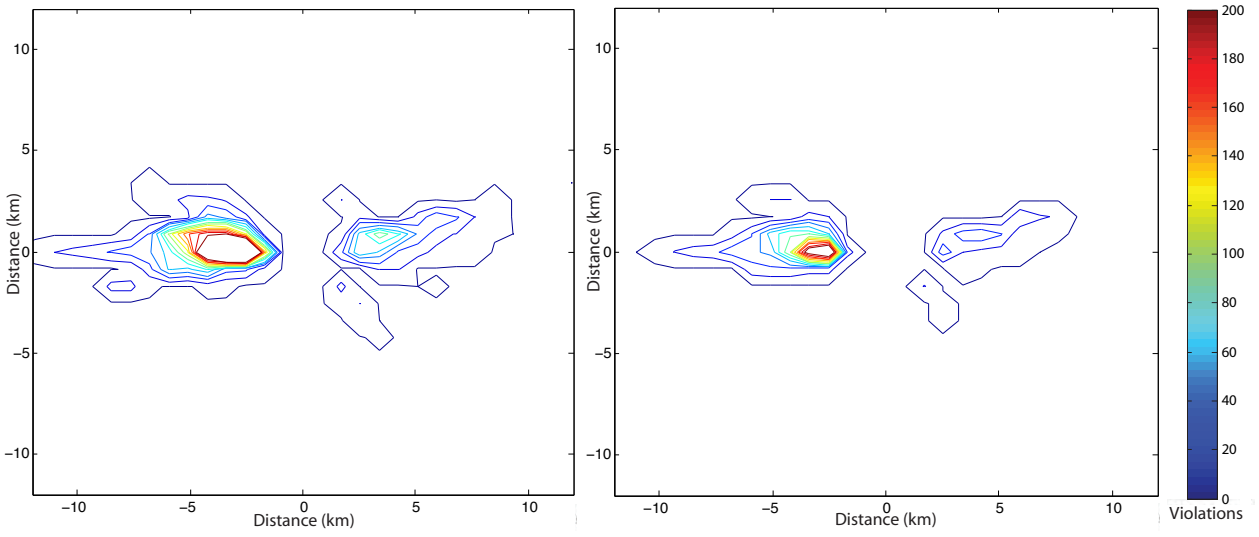

(a) $\dot{m}_s$=245 kg/hr (b) $\dot{m}_s$=210 kg/hr

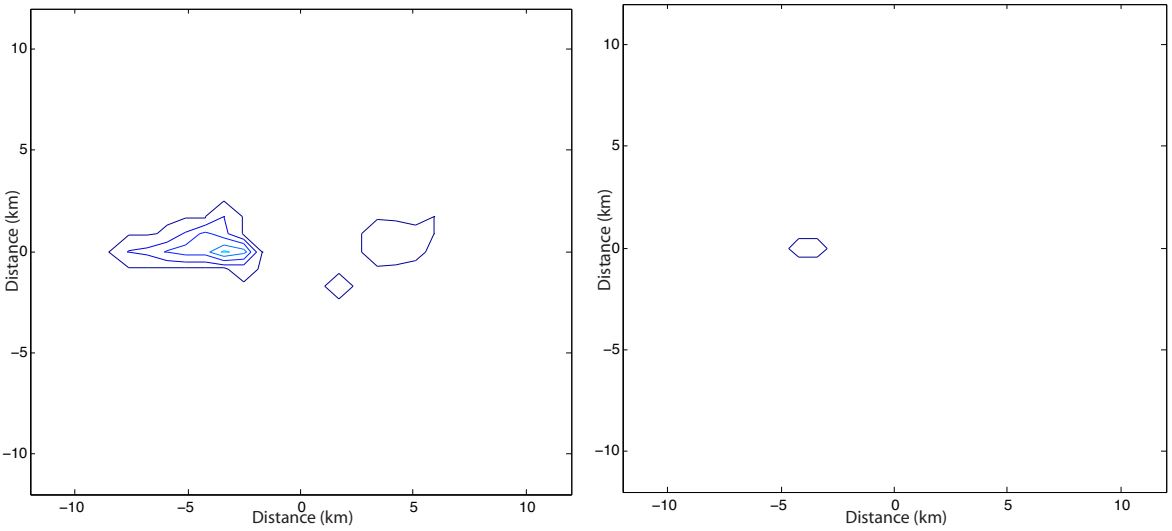

(c) $\dot{m}_s$=175 kg/hr (d) $\dot{m}_s$=122.5 kg/hr

Figure 7: These plots show isoviolation contour maps as $\dot{m}$ is decreased. The goal was to find the minimum $\dot{m}_s$ that created a violation. (d) shows the minimum $\dot{m}_s$ to obtain a violation. (a) is similar to the base case. All Length scales are in km. Contours are at 1:15:200 violations.

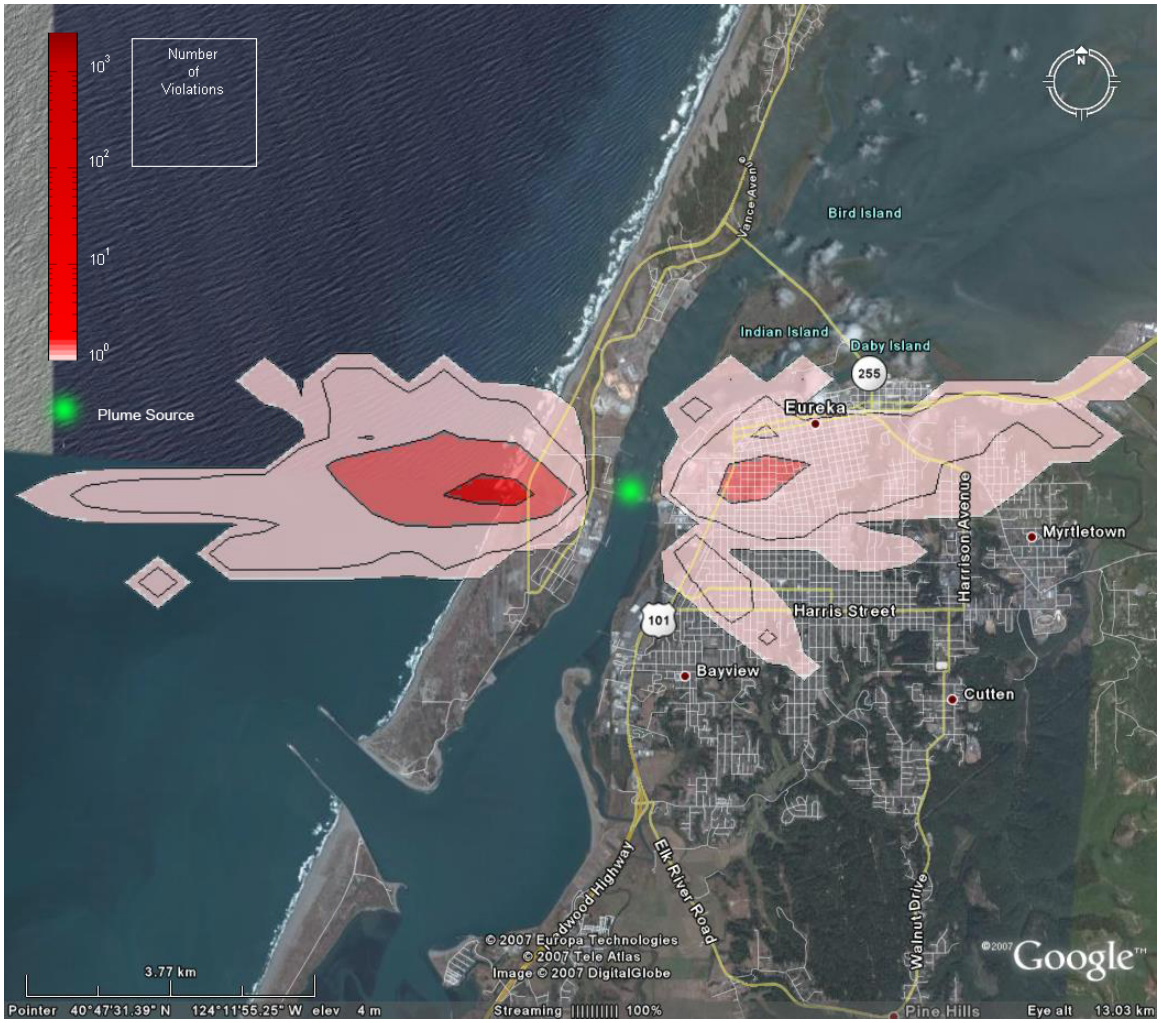

Figure 8: Total number of violations at ground level (z=0m) over a one year simulation with $\dot{m} = 350$ g/hr. The contours are logarithmic, 1:10:100:1000

5.1 Sensitivity

A base case of $\dot{m}_s$=262.5 kg/hr was used to investigate the sensitivity of the model to its parameters. The base case had 125 violation days. The most sensitive parameter was the actual stack height, h_s. The stack height has a direct impact on the effective stack height and the wind speed at the center line of the plume. If the effective stack height is lower, then the concentration at the ground is greater and more violations occur. Variations in the stack tip diameter, d_s and the stack exit velocity, v_s also had significant impacts on the number of violation days. These parameters affect whether the exiting PM_{10} is driven by buoyancy or momentum, and this affects the effective stack height parameter. The effluent exit temperature and the height at which the concentrations were measured, z^* had almost no effect on the number of violation days. The temperature had a small effect suggesting either that momentum forces always dominated the plume rise or that buoyancy rise is insensitive to temperature.

Table 2: To investigate the sensitivity of model, parameters were varied by 20% and the resulting number of violation days were determined. The base case produced 125 violation days.

Parameter	Variation	Violation Days	% Change from Base
d_s	+20%	75	−40.0%
	−20%	211	68.8%
T_s	+20%	125	0.0%
	−20%	126	0.8%
v_s	+20%	98	−21.6%
	−20%	171	36.8%
terrain	rural	97	−22.4%
h_s	+20%	31	−75.2%
	−20%	251	100.8%
z^*	+3m	134	7.2%
	+6m	127	1.6%

6 Conclusions

With a typical auxiliary engine on a large ship docked in Humboldt Bay, CA and running continuously over a year's variation in weather, there would be no violation of the California EPA air quality standard regarding PM_{10} emissions. The predicted concentrations of PM_{10} on the ground in the vicinity of the ship would be under the standard by two orders of magnitude. To cause an air quality violation with regard to PM_{10} would require an output flow rate of approximately 350 times as much PM_{10} as a typical auxiliary engine would output. This might be possible with many more ships, but the current model can not be scaled up to investigate this possibility as multiple ships would no longer be able to be modelled as a point source. If the model were changed to account for multiple sources, it is still likely to require more ships than could fit in the docks in Humboldt Bay before any PM_{10} air quality violations would occur.

Appendix A Plume Rise Formulae

A plume emitted from a stack may rise, fall, or stay roughly at the same height depending on the exit velocity of the gas, the diameter of the stack, the stack gas temperature, the ambient air temperature, and the stability category of the atmosphere [Altwicker 2000]. The height at which the plume stabilizes is called the effective stack height. This height is assumed to contain the centerline of the plume (Figure 1). The following formulae were originally developed by Briggs and were combined in the following manner by the US EPA [1995].

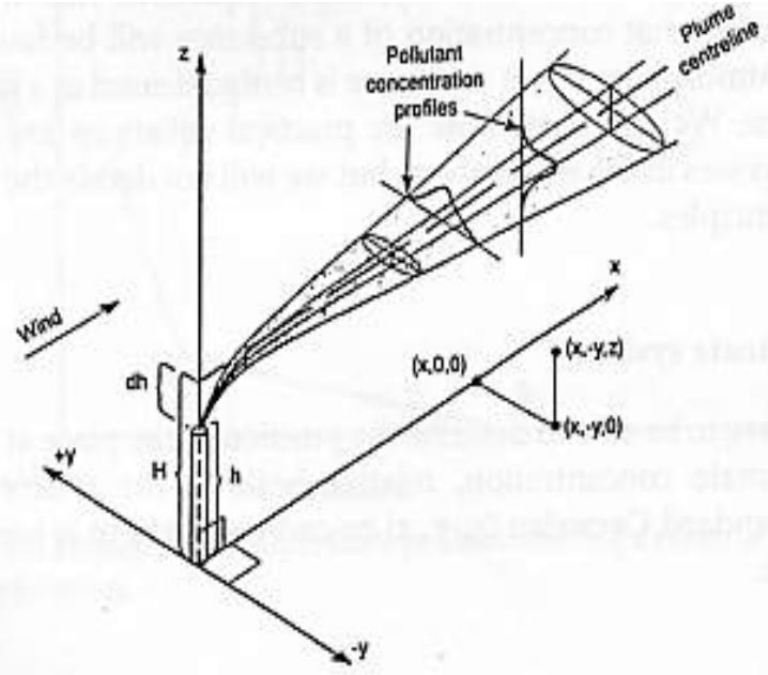

Figure A-1: An idealized plume centered at the final rise height.

The plume rise height is approximated by first determining whether buoyancy or momentum forces dominate the motion of the gas after exiting the stack. If the temperature of the gas is less than the ambient temperature, momentum forces are assumed to dominate. If the temperature of the gas is greater than the ambient temperature, the temperature at which buoyancy forces begin to dominate, T_c, must be calculated using one of two stability dependent expressions [USEPA 1995]:

Unstable or Neutral Formula

$$\text{for } F_b < 55, \quad T_c = (0.0297)\, T_s \left(\frac{v_s^{1/3}}{d_s^{2/3}} \right) \tag{22}$$

$$\text{for } F_b \geq 55, \quad T_c = (0.00575)\, T_s \left(\frac{v_s^{2/3}}{d_s^{1/3}} \right) \tag{23}$$

$$F_b = g v_s d_s^2 \left(\frac{T}{4 T_s} \right) \tag{24}$$

where

F_b = the buoyancy flux term (m^4/s^3)
T_c = crossover temperature above which buoyancy forces dominate (K)
T = difference between stack temperature and ambient temperature (K)
T_s = temperature of the stack (K)
v_s = exit velocity of the gas (m/s)
d_s = stack diameter (m)
g = acceleration due to gravity (m/s^2)
s = stability parameter (K/m)

Stable Formula

$$T_c = 0.019582 T_s v_s \sqrt{s} \quad (25)$$
$$s = 0.020 \text{ K/m}, \quad \text{for stability class E} \quad (26)$$
$$s = 0.035 \text{ K/m}, \quad \text{for stability class F} \quad (27)$$

where

s = stability parameter (K/m)

If the difference between the gas temperature and the stack temperature is greater than T_c, the plume motion is assumed to be buoyancy dominated. Otherwise, momentum is assumed to dominate. Briggs formulae are used to calculate the effective stack height (h_e) and the horizontal distance travelled by the plume (x_f) before attaining the effective stack height. The formulae are different depending on which transport mechanism dominates as well as which stability category is present [USEPA 1995].

Unstable or Neutral - Buoyancy Rise

$$\text{for } F_b < 55, \quad h_e = h_s + 21.425 \left(\frac{F_b^{3/4}}{u_s} \right) \quad (28)$$
$$\text{for } F_b \geq 55, \quad h_e = h_s + 38.71 \left(\frac{F_b^{3/5}}{u_s} \right) \quad (29)$$
$$(30)$$
$$\text{for } F_b < 55, \quad x_f = 49 F_b^{5/8} \quad (31)$$
$$\text{for } F_b \geq 55, \quad x_f = 119 F_b^{2/5} \quad (32)$$

where

h_e = effective stack height (m)
h_s = actual stack height (m)
u_s = wind speed at the stack height (m/s)
x_f = downwind distance to final plume rise (m)

Unstable or Neutral - Momentum Rise

$$h_e = h_s + 3d_s\left(\frac{v_s}{u_s}\right) \tag{33}$$

Stable - Buoyancy Rise

$$h_e = h_s + 2.6\left(\frac{F_b}{u_s s}\right)^{1/3} \tag{34}$$

$$x_f = 2.0715\frac{u_s}{\sqrt{s}} \tag{35}$$

Stable - Momentum Rise

$$h_e = h_s + 1.5\left(\frac{F_m}{u_s\sqrt{s}}\right)^{1/3} \tag{36}$$

$$F_m = v_s^2 d_s^2 \frac{T_a}{4T_s} \tag{37}$$

where

F_m = the momentum flux term (m^4/s^3)

Lastly, the intermediate height of the plume before it has reached the effective stack height can be estimated for buoyancy dominated plume under all stability conditions by the following formula [USEPA 1995].

$$h_e = h_s + 1.60\left(\frac{F_b^{1/3}x^{2/3}}{u_s}\right) \tag{38}$$

where

x = downwind distance (m)

For momentum dominated plume rise, the intermediate plume height is calculated as follows [USEPA 1995].

$$\text{for unstable or neutral,} \quad h_e = h_s + \left(\frac{3F_m x}{\beta_j^2 u_s^2}\right)^{1/3} \tag{39}$$

$$\text{for stable,} \quad h_e = h_s + \left(3F_m\frac{sin(x\sqrt{s}/u_s)}{\beta_j^2 u_s\sqrt{s}}\right)^{1/3} \tag{40}$$

$$\beta_j = \frac{1}{3} + \frac{u_s}{v_s} \tag{41}$$

where

β_j = jet entrainment coefficient (dimensionless)

Appendix B Empirical Constants

Stability classes.

Table B-1: A key to determining Pasquill stability categories [Turner 1970].

Surface Wind Speed (at 10 m) (m/sec)	*Day*			*Night*	
	Incoming Solar Radiation				
	Strong	*Moderate*	*Slight*	*Thinly Overcast or ≥4/8 Low Cloud*	*Clear or ≤3/8 Cloud*
<2	*A*	*A–B*	*B*		
2–3	*A–B*	*B*	*C*	*E*	*F*
3–5	*B*	*B–C*	*C*	*D*	*E*
5–6	*C*	*C–D*	*D*	*D*	*D*
>6	*C*	*D*	*D*	*D*	*D*

Wind profile exponents

Table B-2: Wind speed profile exponents for use in wind power law [USEPA 1995].

Stability Category	Rural Exponent	Urban Exponent
A	0.07	0.15
B	0.07	0.15
C	0.10	0.20
D	0.15	0.25
E	0.35	0.30
F	0.55	0.30

Dispersion coefficients

Table B-3: A formula and corresponding parameter values for determining the lateral diffusion coefficient for a Gaussian plume [USEPA 1995].

PARAMETERS USED TO CALCULATE PASQUILL-GIFFORD σ_y

$$\sigma_y = 465.11628\ (x) \tan(TH)$$

$$TH = 0.017453293\ [c - d\ \ln(x)]$$

Pasquill Stability Category	c	d
A	24.1670	2.5334
B	18.3330	1.8096
C	12.5000	1.0857
D	8.3330	0.72382
E	6.2500	0.54287
F	4.1667	0.36191

where σ_y is in meters and x is in kilometers

Table B-4: A formula and corresponding parameter values for determining the vertical diffusion coefficient for a Gaussian plume [USEPA 1995].

PARAMETERS USED TO CALCULATE PASQUILL-GIFFORD σ_z

		σ_z(meters) = ax^b (x in km)	
Pasquill Stability Category	x (km)	a	b
A*	<.10	122.800	0.94470
	0.10 - 0.15	158.080	1.05420
	0.16 - 0.20	170.220	1.09320
	0.21 - 0.25	179.520	1.12620
	0.26 - 0.30	217.410	1.26440
	0.31 - 0.40	258.890	1.40940
	0.41 - 0.50	346.750	1.72830
	0.51 - 3.11	453.850	2.11660
	>3.11	**	**
B*	<.20	90.673	0.93198
	0.21 - 0.40	98.483	0.98332
	>0.40	109.300	1.09710
C*	All	61.141	0.91465
D	<.30	34.459	0.86974
	0.31 - 1.00	32.093	0.81066
	1.01 - 3.00	32.093	0.64403
	3.01 - 10.00	33.504	0.60486
	10.01 - 30.00	36.650	0.56589
	>30.00	44.053	0.51179

* If the calculated value of σ_z exceed 5000 m, σ_z is set to 5000 m.

** σ_z is equal to 5000 m.

Table B-5: Continuation of figure Appendix B: A formula and corresponding parameter values for determining the lateral diffusion coefficient for a Gaussian plume [USEPA 1995].

PARAMETERS USED TO CALCULATE PASQUILL-GIFFORD σ_z

Pasquill Stability Category	x (km)	σ_z(meters) = ax^b (x in km) a	b
E	<.10	24.260	0.83660
	0.10 - 0.30	23.331	0.81956
	0.31 - 1.00	21.628	0.75660
	1.01 - 2.00	21.628	0.63077
	2.01 - 4.00	22.534	0.57154
	4.01 - 10.00	24.703	0.50527
	10.01 - 20.00	26.970	0.46713
	20.01 - 40.00	35.420	0.37615
	>40.00	47.618	0.29592
F	<.20	15.209	0.81558
	0.21 - 0.70	14.457	0.78407
	0.71 - 1.00	13.953	0.68465
	1.01 - 2.00	13.953	0.63227
	2.01 - 3.00	14.823	0.54503
	3.01 - 7.00	16.187	0.46490
	7.01 - 15.00	17.836	0.41507
	15.01 - 30.00	22.651	0.32681
	30.01 - 60.00	27.074	0.27436
	>60.00	34.219	0.21716

Appendix C Ship Emission Rates

Table C-1: Specifications of Ship and Auxiliary Engines Data [Cooper 2003]

Ship Type	Engine Type	Engine Size (max HP)
Pass. ferry (155m by 29m)	Sulzer	1287
Pass. ferry (175m by 29m)	Sulzer	1703
Pass. ferry (185m by 27m)	Wartsila	1261
Vehicle carrier (199m by 32m)	Wartsila	1985
Container/ ro-ro (292m by 32m)	Wartsila	3587
Chemical tanker (115m by 18m)	Caterpillar	966

Table C-2: Specifications of Ship and Mass Flux Data [Cooper 2003, BAAQMD2007]

Ship Type	Mass Flux [with TBACT stdr.] (g/hr)	Mass Flux [from Cooper] (g/hr)
Pass. ferry	193	89-246
Pass. ferry	255	224-309
Pass. ferry	189	105-189
Vehicle carrier	298	104-129
Container/ ro-ro	538	419-709
Chemical tanker	145	55-72

Appendix D Dose-Response of PM_{10}

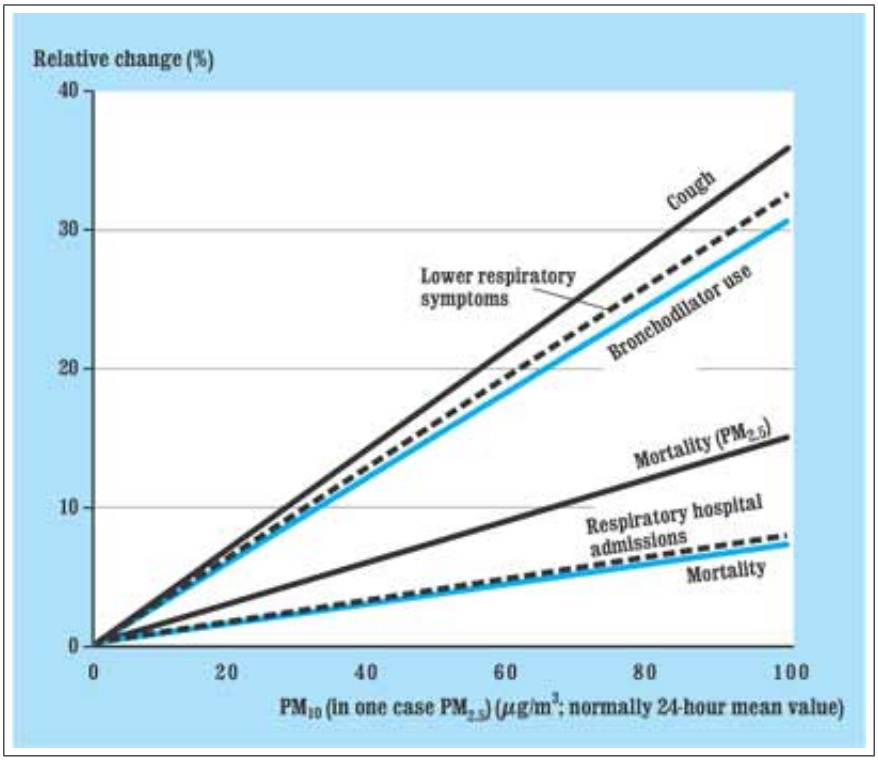

Figure D-1: Link between particles in ambient air and effects on health. Dose response link at exposures below 20 $\mu g/m^3$ is uncertain. [Elvingson and Ågren 2007].

References

Altwicker, E. R. e. a. (2000). *Air Pollution*. Lewis Publishers.

ARB (2007). "Ambient air quality standards (aaqs) for particulate matter." *Url*, California Environmental Protection Agency: Air Resources Board. http://www.arb.ca.gov/research/aaqs/pm/pm.htm.

BAAQMD (2007). "Engineering evaluation report: Moody's kmv." *Url*, Bay Area Air Quality Managment District. http://www.baaqmd.gov/pmt/public_notices/2003/6496/B4996_nsr_6496_eval_021103.pdf.

Calhoun-Lopez, M. and Gunzburger, M. D. (2005). "A finite element, multiresolution viscosity method for hyperbolic conservation laws." *SIAM Journal on Numerical Analysis*, 43(5), 1988–2011.

Carbon, B. (2003). "Health effects of pm10 in new zealand." *Technical report no. 39*, Ministry of the Environment on Air Quality, New Zealand.

Chapra, S. C. and Canale, R. P. (2006). *Numerical Methods for Engineers*. McGraw-Hill, 5^{th} edition.

Cooper, D. (2003). "Exhaust emissions from ships at berth." *Atmospheric Environment*, 37, 3817–3810.

CSU (2007). "Off shore emmissions." *Url*, Colorado State University. vista.cira.colostate.edu/docs/wrap/emissions/OffshoreEmissions.doc.

Elvingson, P. and Ågren, C. (2007). "Air and the environment." *Url*, The Swedish NGO Secretariat of Acid Rain. http://www.acidrain.org/pages/publications/AirAndTheEnvironment/AE_chp3.htm.

Genuchten, M. V. and Gray, W. (1978). "Analysis of some dispersion corrected numerical schemes for solution of the transport equation." *International Journal of Numerical Methods in Engineering*, 12, 387–404.

Gipe, P. (2004). *Wind Power*. Chelsea Green Publishing Company, White River Junction, VT.

Horel, J., Splitt, M., Pechmann, J., Olsen, B., and Delgado, E. (2007). "Roman- realtime observation monitoring and analysis network." *Report no.*, NOAA Cooperative Institute for Regional Prediction.

Huebner, K. H., Dewhirst, D. L., Smith, D. E., and Byron, T. G. (2001). *The Finite Element Method for Engineers*. Wiley Interscience.

Janhall, S. (2007). "Particle emissions from ships." *Report no.*, The Alliance For Global Sustainability.

Kitabayashi, K., Konishi, S., and Katatani, A. (2006). "Nox plume dispersion model with chemical reaction in polluted environment." *JMSE International Journal*, 49, 42–47.

Lantz, R. (1971). "Quantitative evaluation of numerical diffusion truncation error." *Society of Petroleum Engineering Journal*, 11, 315–320.

Liu, C. and Leung, D. (1997). "Numerical study of atmospheric dispersion under unstably stratified atmosphere." *Journal of Wind Engineering and Industrial Aerodynamics*, 67-68, 767–779.

Lua, G., Brooka, J. R., Alfarra, M. R., Anlauf, K., Leaitch, W. R., Sharma, S., Wang, D., Worsnop, D. R., and Phinney, L. (2006). "Identification and characterization of inland ship plumes over vancouver, bc." *Atmospheric Environment*, 40, 2767–2782.

MATLAB (2007). "Matlab function reference. `http://www.mathworks.com/access/helpdesk/help/techdoc/index.html?/access/helpdesk/help/ techdoc/ref/mldivide.html`.

Mazzia, A., Bergamaschi, L., and Putti, M. (2000). "A time-splitting technique for the advection-dispersion equation in groundwater." *J. Comput. Phys.*, 157(1), 181–198.

Nepf, H. (2004). "Advection and diffusion of an instantaneous, point source." *Report no.*, Mit Open Courseware.

Ninga, Z., Cheungb, C., Lua, Y., Liub, M., and Hungc, W. (2005). "Experimental and numerical study of the dispersion of motor vehicle pollutants under idle condition." *Atmospheric Environment*, 39, 7880–7893.

Sayma, A. and Betts, P. (1997). "A finite element model for the simulation of dense gas dispersion in the atmosphere." *International Journal for Numerical Methods in Fluids*, 24, 291–317.

Schwarz, K. T., Patzek, T. W., and Silin, D. B. (2006). "On prediction of wind-borne plumes with simplemodels of turbulent transport." *Report no.*, Lawrence Berkeley National Laboratory.

Socolofsky, S. A. (2002). "Environmental fluid mechanics part i: Mass transfer and diffusion." *Report no.*, IFH.

Tkalich, P. and Chan, E. S. (2003). "The third-order polynomial method for two-dimensional convection and diffusion." *International Journal for Numerical Methods in Fluids*, 41, 997–1019.

Turner, D. (1970). *Workbook of atmospheric dispersion estimates (Revised)*. US EPA: Office of Air Programs, Research Triangle Park, N.C. Pub. No. AP-26.

UKNEAI (2007). "Pm_{10}." *Url*, The UK Emission Factor Database. `http://www.naei.org.uk/pollutantdetail.php?poll_id=24`.

USEPA (1995). *User's guide for the Industrial Source Complex (ISC3) Dispersion Models*. US EPA: Office of Air Quality Planning and Standards Emissions, Monitoring, and Analysis Division, Research Triangle Park, N.C. Vol. 2, EPA-454/B-95-003b.

Wang, H. and Lacroix, M. (1997). "Optimal weighting in the finite difference solution of the convection-dispersion equation." *Journal of Hydrology*, 200, 228–242.

Wang, H. F. and Anderson, M. P. (1982). *Introduction to Groundwater Modeling: Finite Difference and Finite Element Methods*. W. H. Freeman and Company.

Willis, R. (2007). "Personal communication. Humboldt State University.

Willis, R. and Yeh, W. W.-G. (1987). *Groundwater Systems Planning and Management*. Prentice-Hall, Inc., Englewood Cliffs, New Jersey, 1^{st} edition.